PHYSICAL REVIEW B, VOLUME 63, 100406(R)

Electron doping in $CaMnO_3$ induced by Mo for Mn substitution: An efficient route to orbital and charge ordering

C. Martin, A. Maignan, M. Hervieu, and B. Raveau
Laboratoire CRISMAT, UMR 6508 CNRS ISMRA et Université de Caen, 6 boulevard Maréchal Juin, 14050 Caen cedex, France

J. Hejtmanek
Institute of Physics of ASCR, Cukrovarnicka 10, 16200 Praha 6, Czech Republic

(Received 8 August 2000; revised manuscript received 28 November 2000; published 21 February 2001)

The magnetic, transport, and structural investigations of the $CaMn_{1-x}Mo_xO_3$ manganites show that orbital and charge ordering are induced by Mn-site doping in pure calcium based manganites. Starting from a cluster glass behavior at $x \approx 0.04$, orbital ordering is evidenced for $x \approx 0.10$, whereas charge ordering (characterized by an incommensurate structure with $q \approx 0.02$–0.25) is obtained for $x \approx 0.12$ with a high-$T_{Co} \approx 300$ K. This charge ordering effect induced by Mo doping is interpreted in terms of a high valency effect.

DOI: 10.1103/PhysRevB.63.100406 PACS number(s): 75.25.+z, 71.30.+h, 68.37.−d

The issue of charge ordering (CO) in the manganites $Ln_{1-x}Ca_xMnO_3$ (Ln=lanthanide) is of great importance since this phenomenon has a prominent role in the appearance of the antiferromagnetic (AFM) state at low temperature, and consequently influences the colossal magnetoresistance (CMR) properties of these materials. First observed for the half doped manganites,[1–8] CO was shown to exist for other compositions, appearing in the form of single Mn^{3+} stripes alternating with blocks of Mn^{4+} stripes (or layers), depending on the x value.[7,9] Each of these CO structures is modulated, either commensurate or incommensurate, and characterized by a q modulation vector, closely related to the composition, $q \approx 1-x$, which corresponds to the long-range ordered distribution of the stripes. Such ordered stripes are responsible for the AFM ordering of the spins derived from the CE-type structure, depending on x.

The melting of this CO state under a magnetic field, generally observed for $x<0.50$, is at the origin of the CMR effect, due to the collapse of the AFM-CO regions which coexist with ferromagnetic metallic (FMM) regions at low temperature LT.[10–15] Actually, the CO state stability is closely related to the average size of the a-site cation, decreasing as $\langle r_A \rangle$ increases.[16–19] Another way of weakening the CO state and inducing ferromagnetism and metallicity consists of doping the Mn site with a magnetic cation such as Cr, Co, Ni, or Ru.[20–23] From a more general viewpoint, it is now currently admitted that the doping of the Mn site by a foreign cation, whatever its nature, induces disorder on the Mn sites, and consequently destroys charge ordering.[21–23] We report herein on the opposite effect, i.e., CO induced by Mn site substitution, in the $CaMn_{1-x}Mo_xO_3$ series. Starting from the G-type antiferromagnet $CaMnO_3$, the substitution of Mo for Mn first induces a ferromagnetic cluster glass for lower doping levels ($x \leqslant 0.04$),[24] and then we show that beyond a certain doping level of molybdenum, orbital ordering (OO) and then CO are established.

The preparation of the $CaMn_{1-x}Mo_xO_3$ samples ($0 \leqslant x \leqslant 0.15$) has been previously reported.[25] In this range, the Mo substitution, as analyzed by x-ray energy dispersive spectroscopy coupled to electron diffraction (ED) is highly homogeneous (± 0.01) around the Mo content, equal to the nominal content (x). The magnetic behavior has been probed by ac susceptibility [$h_{ac}=3$ Oe and $f=100$ Hz] whereas the electronic properties have been studied using four-probe resistivity, thermoelectric (Seebeck), and thermal conductivity measurements in a quantum design physical properties measurements system (PPMS) (5–400 K up to 9 T). Electron microscopy study has been made with a JEOL 2010 electron microscope, operating between 92 and 370 K.

The curves $\chi'(T)$ (Fig. 1) of the $CaMn_{1-x}Mo_xO_3$ samples corresponding to $x=0.07$ and $x=0.12$ clearly show that an AFM state replaces the weak FM state previously observed[24] for lower doping levels ($x \approx 0.02$–0.04). In the $x=0.07$ and 0.12 curves, ac-susceptibility maxima are observed at 160 and 300 K, respectively. They are reminiscent of similar curves observed for other manganites, which exhibit a structural transition induced by charge and orbital ordering.[6–9,25–27]

The structural transitions of these $CaMn_{1-x}Mo_xO_3$ compositions have been studied by electron microscopy as a function of temperature. For $x=0.07$, a transition is observed at 160 K from the orthorhombic Pnma-type structure with ''$a_p\sqrt{2} \times 2a_p \times a_p\sqrt{2}$'' at room temperature [Fig. 2(a)] to a monoclinic structure with (''$a_p\sqrt{2} \times 2a_p \times a_p\sqrt{2}$'' and $\beta = 90° - \varepsilon$) and $P2_1/m$ space group below 160 K [Fig. 2(b)].

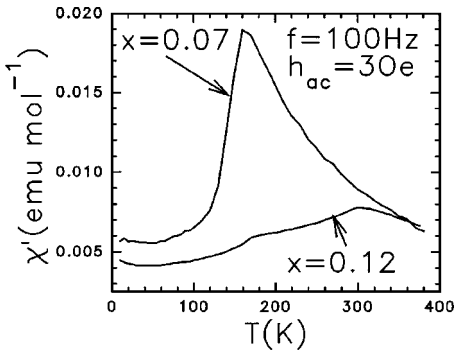

FIG. 1. T dependence of the real part (χ') of the ac-χ for $CaMn_{1-x}Mo_xO_3$ samples with $x=0.07$ and $x=0.12$. x values are labeled on the graph.

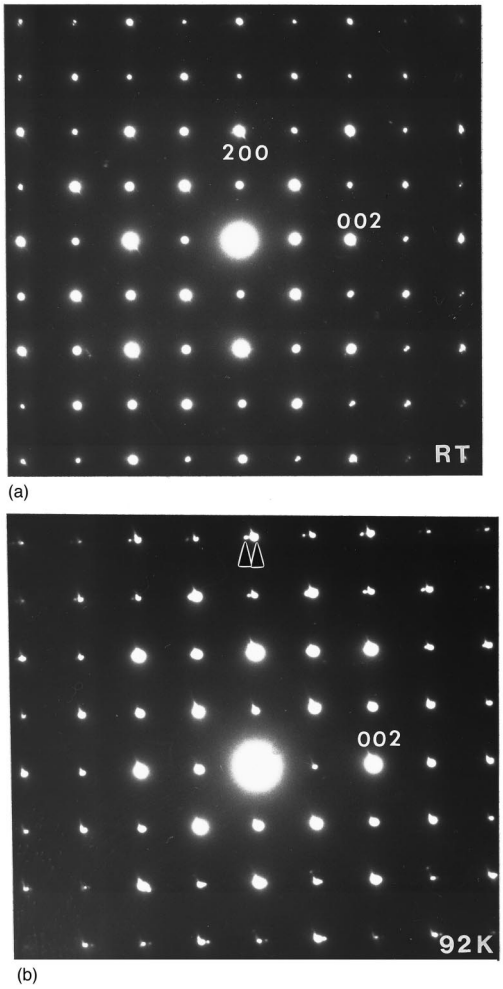

FIG. 2. $x=0.07$. [010] electron diffraction patterns recorded at (a) RT and (b) 92 K. The splitting of the reflections is characteristic of the monoclinic distortion of the cell (see small arrows).

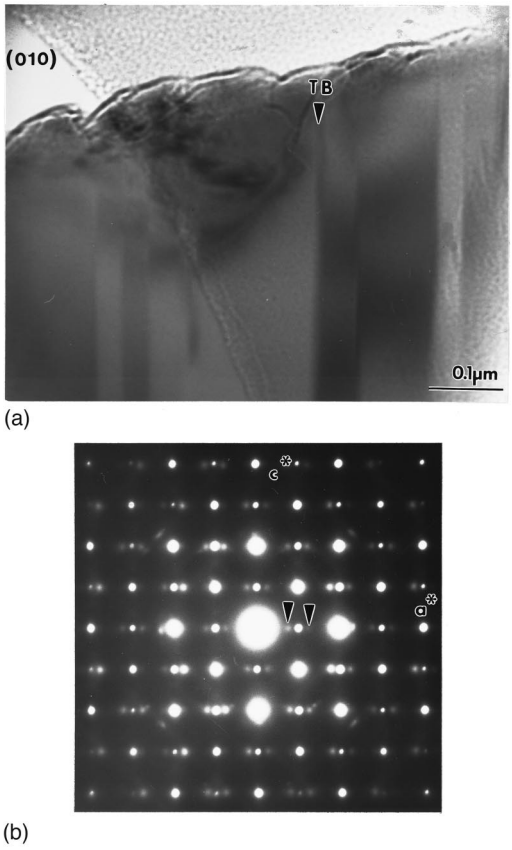

FIG. 3. $x=0.12$. (a) RT [010] bright field image showing a monoclinic area with twinning domains (one twinnning domain is indicated by a small arrow). (b) RT [010] ED pattern of an ordered area. The modulation vector is parallel to a^* and satellites (see small arrows) are the signature of a charge/orbital ordering phenomenon.

In the 92 K [010] ED patterns, a splitting of the reflections (see small arrows) is observed, characteristic of the formation of twinning domains due to the monoclinic distortion. In this manganite, no extra spots are detected whatever T. Thus, the $x=0.07$ sample exhibits a monoclinic distortion at 160 K which is similar to that observed in the C-type AFM structure.[25,27] In this magnetic structure, though no CO is evidenced, the e_g orbitals of manganese are polarized along chains making the OO. As aforementioned, the EDS analyses of the $x=0.12$ sample confirm the x value and the homogeneity of the sample. In contrast, the [010] ED patterns evidence the coexistence of three structural types from 92 K up to 290 K as illustrated in Fig. 3 by the 290 K patterns. The first one is a monoclinic structure (''$a_p\sqrt{2}\times 2a_p \times a_p\sqrt{2}$'' and $\beta=90°-\varepsilon$) with twinning domains [Fig. 3(a)], as described above for the x values close to 0.1. The parameters of the second structure are similar (''$a_p\sqrt{2}\times 2a_p \times a_p\sqrt{2}$'' and $\beta=90°$) but the ED patterns show cross-shaped reflections, the cross arms being elongated along the [100]* and [001]* directions. This phenomenon is characteristic of a so-called tweed structure. The third structural type, which is that of the majority phase, exhibits extra reflections in incommensurate positions. This system of satellites is characteristic of a CO state, with a modulation vector qa^*, with q values ranging between 0.20 and 0.25 [Fig. 3(b)]. The supercell, with ''$(1/q)a_p\sqrt{2}\times 2a_p\times a_p\sqrt{2}$,'' is similar to those observed for the CO $Ln_{1-x}Ca_xMnO_3$ manganites with $x\approx 0.75$.[7,9] Such a structure can be described by the regular stacking of four Mn planes, in which one Mn^{3+} plane alternates with three Mn^{4+} planes. In these structures, the CO is driven by 90° arrangements of the $Mn^{3+}d_z^2$ orbitals and consequently the CO and OO occur simultaneously. The different crystallite types were then warmed keeping constant the electron current density (≈ 80 pA.cm^{-2}). On one hand, in the minority monoclinic and tweed regions the transitions to the orthorhombic structure (*Pnma*) are abrupt and occur at about the same temperature value of 295 K. On the other hand, for the majority charge-ordered regions the transition temperature range is broader. The satellites weaken and become streaky as T increases from 290 K. At 300 K they are scarcely visible and thus $T_{CO}\approx 300$ K.

The electron microscopy results demonstrate that the maximum of $\chi'(T)$ at 300 K (Fig. 1) observed for the $x=0.12$ sample corresponds to structural transitions at T_{CO} ($=T_{OO}$). One remarkable feature concerns the different

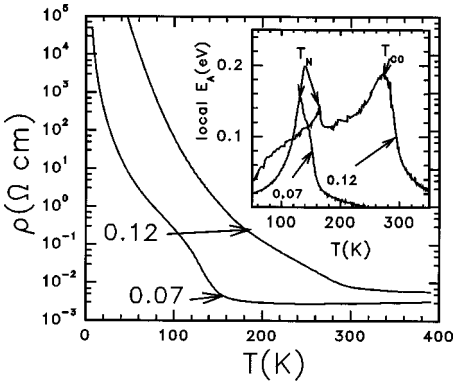

FIG. 4. T dependence of the resistivity (ρ) for the samples $CaMn_{1-x}Mo_xO_3$. x values are labeled on the graph. Inset: Local activation energy $d \ln \rho / dT^{-1}$ vs T for the corresponding $x=0.07$ and $x=0.12$ samples.

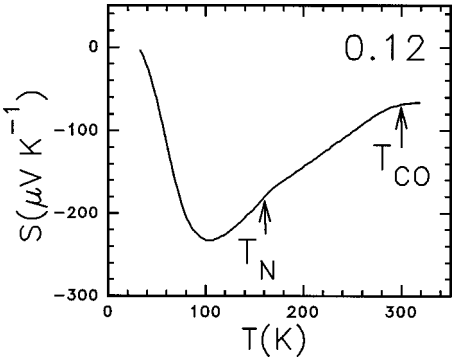

FIG. 5. T-dependent thermopower of $CaMn_{0.88}Mn_{0.12}O_3$ ($x=0.12$). The transition temperatures of CO (T_{CO}) and AFM (T_N) are indicated on the graph.

shape of the $\chi'(T)$ curves of the $x=0.12$ sample, compared to the $x=0.07$ one. Only one maximum is observed for $x=0.07$, whereas for $x=0.12$, an additional change of slope is observed (Fig. 1) at 160 K. This shoulder one the $\chi'(T)$ curve can be attributed to the appearance of long-range AFM ordering (see below). Consequently for $x=0.07$, the appearance of AFM coincides with orbital ordering ($T_N \approx T_{OO}$), whereas for $x=0.12$ AFM appears at a lower temperature than charge ordering ($T_N < T_{CO} = T_{OO}$).

The $\rho(T)$ curves (Fig. 4) are consistent with the above statements. The $x=0.07$ and $x=0.12$ samples exhibit a metal to insulator transition at decreasing temperature, T_{MI} coinciding with the temperature of the maxima of the $\chi'(T)$ curves, i.e., with T_{OO} or T_{CO}/T_{OO}. Thus, T_{MI} increases dramatically as x increases, from 160 K for $x=0.07$ up to 300 K for $x=0.12$. Note also that the $\rho_{390\ K}$ values increase as the Mo content (x) increases, as expected if one refers to the impurity scattering process. To illustrate more clearly the observed ρ discontinuities, the temperature dependence of the local activation energy, defined as $W_{local} = d \ln \rho / d(1/T)$, is given in the inset of Fig. 4. For the $x=0.07$ sample, a single peak of W_{local} is observed with a maximum at 132 K and a minor shoulder at 145 K. For higher Mo content, i.e., for $x=0.12$ in Fig. 4, a double peak feature of W_{local} is obtained and the temperature difference between the peaks increases consistently with the decoupling of CO (T_{CO}) and spin ordering (T_N).

The evolution of the magnetic and transport properties of these $CaMn_{1-x}Mo_xO_3$ oxides mimics remarkably the behavior previously reported for the $Sm_{1-y}Ca_yMnO_3$ series.[28–30] It can be explained by the injection of electrons (increase of Mn^{3+} content) in the $CaMnO_3$ matrix, according to the charge equation $3\ Mn^{4+} = Mo^{6+} + 2\ Mn^{3+}$ of the substitution reaction, whereas in the $Sm_{1-y}Ca_yMnO_3$ system, electrons (Mn^{3+}) are introduced by the replacement of Ca^{2+} by Sm^{3+}. A cluster glass behavior is observed in both systems at very close Mn^{3+} content (0.10 Mn^{3+} per Mn site) corresponding to $x \approx 0.04$ and $y \approx 0.90$, respectively. In the same way, charge ordering appears beyond a Mn^{3+} concentration which is the same, namely 0.20 Mn^{3+} per Mn site, in both system corresponding to $x=0.10$ and $y=0.80$, respectively. Finally it is worth pointing out that the q value of 0.20–0.25 observed at room temperature for $x=0.12$ is in perfect agreement with the theoretical value of 0.24 expected for such a $Ca[Mn^{3+}_{0.24}Mn^{4+}_{0.64}Mo^{6+}_{0.12}]O_3$ composition.

To further elucidate the transport properties, thermoelectric power measurements were carried out. The different characteristic temperatures, T_{OO} and T_N are identified for $x=0.12$ in Fig. 5 coherently with the resistivity data (Fig. 4). For this composition, the negative value of thermopower at high temperature agrees with an electronlike conduction in the bottom of spin polarized Mn e_g − O $2p\sigma^*$ band. The high absolute value, unusual for a classical metallic picture, can be interpreted as a simultaneous impact of relatively small band filling, which shifts the Fermi energy to band edge, and electron correlations: two effects which coherently should increase the small bare metallic thermopower. This metallic behavior is hardly observed since below $T_{CO} \approx 300$ K the thermopower starts to decrease. We interpret this decrease, in agreement with resistivity and ED data, as a consequence of carrier localization due to the CO/OO effect. Then a change of slope with a further decay below 170 K (T_N) is observed. Below T_N when the temperature is lowered, it reaches a minimum of $-230\ \mu$V/K at about 100 K, and finally increases abruptly below this temperature to reach $\approx 0\ \mu$V/K at 10 K.

In summary, all these results show the possibility to induce orbital ordering by substituting Mo^{6+} species for Mn^{4+} in $CaMnO_3$. But more importantly, charge ordering induced by Mn-site substitution is evidenced, Mn-site substitution made by different authors leading to the opposite, i.e., the destruction of CO due to the disorder on the Mn site. Moreover, it is remarkable that charge ordering develops at unusually high temperature, T_{CO} reaching 300 K for $CaMn_{0.88}Mn_{0.12}O_3$, a temperature significantly larger than the maximum temperature of 280 K observed in the $Sm_{1-x}Ca_xMnO_3$ system.[7,19,30] The high valency of molybdenum (Mo^{6+}) can explain its exceptional ability to induce charge ordering. It allows the crucial Mn^{3+} level (0.20–0.25 Mn^{3+} per Mn) required for CO to be reached, using a minimum of Mo^{6+} species (0.12 Mo^{6+} per Mn) so that the Mn lattice is not highly disturbed. It is possible that the similar ionic radius for Mo^{6+} and Mn^{4+} does not affect too much the

formation of the majority Mn^{4+} planes in the CO structures. Finally, doping of Mn sites by Mo^{6+} avoids the size mismatch and eventual magnetic interactions on the *A* site, which is sometimes encountered in $Ln_{1-x}Ca_xMnO_3$ manganites, so that the ordering of orbitals and charges can develop freely at higher temperature, being, of course, limited by a critical value of the Mo^{6+} level. This possibility to induced the Mn^{3+}/Mn^{4+} charge ordering in manganites by Mn-site substitutions demonstrates once more the richness and complexity of these materials.

[1] P. M. Woodward, D. E. Cox, T. Vogt, C. N. R. Rao, and A. K. Cheetham, Chem. Mater. **11**, 3528 (1999).
[2] C. H. Chen and S. W. Cheong, Phys. Rev. Lett. **76**, 4042 (1996).
[3] P. Radaelli, D. E. Cox, M. Marezio, and S. W. Cheong, Phys. Rev. B **55**, 3015 (1997).
[4] S. Mori, T. Katsufuji, N. Yamamoto, C. H. Chen, and S. W. Cheong, Phys. Rev. B **59**, 13 573 (1999).
[5] Y. Tomioka, A. Asamitsu, H. Kuwahara, Y. Moritomo, and Y. Tokura, Phys. Rev. B **53**, R1689 (1996).
[6] Z. Jirak, S. Krupicka, Z. Simsa, M. Dlouha, and S. Vratislav, J. Magn. Magn. Mater. **53**, 153 (1985).
[7] M. Hervieu, A. Barnabé, C. Martin, A. Maignan, F. Damay, and B. Raveau, Eur. Phys. J. B **8**, 31 (1999).
[8] K. Liu, X. W. Wu, K. H. Ahn, T. Sulchek, C. L. Chien, and J. Q. Xia, Phys. Rev. B **54**, 3007 (1996).
[9] C. H. Chen, S. W. Cheong, and H. Y. Hwang, J. Appl. Phys. **81**, 4326 (1997).
[10] P. Schiffer, A. P. Ramirez, W. Bao, and S. W. Cheong, Phys. Rev. Lett. **75**, 3336 (1995).
[11] P. G. Radaelli, D. E. Cox, M. Marezio, S. W. Cheong, P. Schiffer, and A. P. Ramirez, Phys. Rev. Lett. **75**, 4488 (1995).
[12] G. Allodi, R. De Renzi, G. Guidi, F. Licci, and M. W. Piepper, Phys. Rev. B **56**, 6036 (1997).
[13] G. Allodi, R. De Renzi, F. Licci, and M. W. Piepper, Phys. Rev. Lett. **81**, 4736 (1998).
[14] N. Fukumoto, S. Mori, N. Yamamoto, Y. Moritomo, T. Katsufuji, C. H. Chen, and S. W. Cheong, Phys. Rev. B **60**, 12 963 (1999).
[15] K. H. Kim, M. Uehera, C. Hess, P. A. Sharma and S. W. Cheong, Phys. Rev. Lett. **84**, 2961 (2000).
[16] N. Kumar and C. N. R. Rao, J. Solid State Chem. **129**, 363 (1997).
[17] A. Barnabé, M. Hervieu, C. Martin, A. Maignan, and B. Raveau, J. Appl. Phys. **84**, 5506 (1998).
[18] F. Damay, C. Martin, A. Maignan, M. Hervieu, B. Raveau, Z. Jirak, G. André, and F. Bouré, Chem. Mater. **11**, 536 (1999).
[19] C. Martin, A. Maignan, M. Hervieu, and B. Raveau, Phys. Rev. B **60**, 12 191 (2000).
[20] B. Raveau, A. Maignan, and C. Martin, J. Solid State Chem. **130**, 162 (1997).
[21] P. V. Vanitha, A. Arulraj, A. R. Raju, and C. N. R. Rao, C. R. Acad. Sci., Ser. IIb: Mec., Phys., Chim., Astron. **2**, 595 (1999).
[22] P. V. Vanitha, R. S. Singh, S. Natarajan, and C. N. R. Rao, J. Solid State Chem. **137**, 365 (1998).
[23] A. Maignan, F. Damay, A. Barnabé, C. Martin, M. Hervieu, and B. Raveau, Philos. Trans. R. Soc. London, Ser. A **356**, 1635 (1998).
[24] B. Raveau, Y. M. Zhao, C. Martin, M. Hervieu, and A. Maignan, J. Solid State Chem. **149**, 203 (2000).
[25] W. Bao, J. D. Axe, C. H. Chen, and S. W. Cheong, Phys. Rev. Lett. **78**, 543 (1997).
[26] M. T. Fernandez-Diaz, J. L. Martinez, J. M. Alonso, and E. Herrero, Phys. Rev. B **59**, 1277 (1999).
[27] C. Martin, A. Maignan, M. Hervieu, B. Raveau, Z. Jirak, A. Kurbakov, V. Trounov, G. André, and F. Bouré, J. Magn. Magn. Mater. **205**, 184 (1999).
[28] C. Martin, A. Maignan, F. Damay, M. Hervieu, and B. Raveau, J. Solid State Chem. **134**, 198 (1997).
[29] A. Maignan, C. Martin, F. Damay, B. Raveau, and J. Hejtmanek, Phys. Rev. B **58**, 2758 (1998).
[30] J. Hejtmanek, Z. Jirak, M. Marysko, C. Martin, A. Maignan, M. Hervieu, and B. Raveau, Phys. Rev. B **60**, 14 057 (1999).